

Results are generalized from an experimental study of the dynamics of a gas jet in a liquid, the structure of the region of interaction, and the regimes of discharge from the submerged nozzle with different degrees of gas assimilation.

The discharge of a gas jet from a submerged nozzle and development of the flow in a liquid have been studied by several authors on model media [1-8] and liquid metals [2, 8-15]. However, the mechanism and laws of interaction in the gas-liquid system are not clear, and the characteristics of the discharge regimes and the region of interaction are to a large extent contradictory. The same is true of the physicochemical parameters governing the process. For example, the literature contains references to more than ten regimes of discharge of the gas from the nozzle. These regimes are differentiated between one another mainly by external signs and they lack physical substantiation. Most investigations regard the region of interaction between the gas jet and the liquid as a stationary region, characterizable by its mean length and diameter. However, even with this simplified approach, there are conflicting opinions on the structure of the flow. Some authors hold that the region is filled with a discrete, low-velocity gas and a gas-liquid medium. Others represent the region in the form of a solid two-phase jet. The works [16, 17] emphasized that the processes of jet development were fully analogous in gas-gas, gas-liquid, and liquid-liquid systems, while other investigators denied the validity of such an analogy.

Also contradictory is the estimate of the effect of the degree of assimilation (absorption) of the gas in the liquid. Proceeding on the basis of theoretical analysis of the interaction process [18] and of experiments with a supply of vapor from a submerged nozzle (M. P. Sobakin and Ya. D. Verbitskii), most authors claim that this parameter has no effect on the structure and dimensions of the interaction region. At the same time, it is shown experimentally in [4, 6] that gas assimilation not only is a quantitative factor, but that it completely restructures the flow in some cases.

These problems made it necessary for us to conduct a comprehensive experimental study of the discharge of a gas jet from a nozzle and its development in a liquid. The study focused on the following: investigation of the mechanism of interaction in the gas-liquid system and evaluation of the effect of the blowing (injection) regimes and degree of gas assimilation on the interaction process; study of the structure and dynamics of the interaction region; determination and substantiation of the gas-jet discharge regimes from the submerged nozzle; construction of a dynamic model of the interaction region with allowance for different gas assimilations.

The tests were conducted in a wide range of injection conditions (nozzles: bottom, lateral, top, sonic-conical and cylindrical, supersonic-Laval, axisymmetric, and plane; injection pressure $P_0 = P_n - 41 \cdot 10^5$ Pa; gas discharge velocity $V_a = 2-1000$ m/sec; $n = 1-20$; $M_a = 0.005-3.0$; $d_0 = 2 \cdot 10^{-3}-50 \cdot 10^{-3}$ m). The model media: nitrogen, air, helium, carbon dioxide (CO_2), chlorine (Cl_2), hydrogen chloride (HCl), ammonia (NH_3), steam superheated to the temperature $T_g = 200-250^\circ C$, water with a temperature $T_q = 18-100^\circ C$, solutions of KOH and NaOH. The coefficient (degree) of assimilation of the gas $A = 0-710$ (m^3 gas/ m^3 liquid). We studied different mechanisms of assimilation (steam + water - phase transformation, Cl_2 (CO_2) + NaOH(KOH) and $NH_3 + H_2O$ - chemisorption, HCl + water - physical absorption). The

fields of excess pressure in the two-phase flow ΔP (the dynamic pressure ρV^2) were measured with preheated and liquid-filled pitot tubes with an outlet to manometers and an inductive apparatus, respectively. Simultaneously with the measurements we observed the flows with a high-speed camera and by spark methods. The results were analyzed statistically by the method in [5]. The data we obtained on "cold" models was compared with the results of experiments on metals [2, 8-15], which allowed us to generalize our conclusions.

Structure of the Interaction Region. Tests conducted with different levels of injection showed that the process of discharge of the gas into the liquid layer is always non-steady, regardless of the orientation of the submerged lance relative to the level of the bath. The tests also showed that the process is governed by the longitudinal and transverse pulsations of the flow. An analysis of the films of the interaction in the gas-liquid system (Fig. 1) shows that there is a region near the nozzle edge which has a complex structure and boundaries that vary with time and space. These boundaries separate the rapidly moving gaseous or two-phase medium from the relatively still body of pure liquid. The composition and structure of the gas flow in the liquid and the dynamics of its boundaries are complex and are quite different from those of gas-gas and gas-liquid systems. This difference is due to a complex of phenomena occurring at the microscopic and macroscopic levels. The flow composition and structure and the dynamics of the boundaries depend significantly on the injection regimes (discharge G_g , P_0 , V_a) and the degree of assimilation of the gas A (Fig. 1). A different orientation of the nozzle edge, not affecting the mechanism of interaction, leads to slight differences. These differences are dependent primarily on the character of interaction of the inertial forces of the flow and buoyancy, as well as on the direction and intensity of the circulation flows in the liquid volume and the presence and features of a bubble region.

Two zones with a characteristic structure can be distinguished in the interaction region: an internal, relatively stable region of jet flow and a peripheral region of pulsating gaseous and two-phase masses (bubbles and cavities). The structure, composition, and dynamics of these zones are determined mainly by the values of the criteria $\bar{P} = P_f/P_0$, A , M_a , n .

Measurements of the excess-pressure fields ΔP (dynamic velocities ρV^2) confirmed the data in [7, 19-21] for slightly assimilated and nonassimilated gases ($A < 10$) on the presence of turbulent jet flow in the internal zone. This jet flow has the initial, transitional, and main sections and corresponding profiles [22] typical of submerged gas jets. The results of our tests with bottom axisymmetric and plane nozzles in the sub- and supersonic regimes amplified the information obtained in [7, 19] on the structure of the jet region in a gas-liquid system. Injection with the lateral and top nozzles used in metallurgy allowed us to generalize the results obtained to the case of discharge of a gas jet from an arbitrarily oriented nozzle.

It can be seen from Fig. 2[†] that for the above conditions, the test points measured at different stations of the main section of the gas jet in the liquid are grouped around the curve proposed by Abramovich for a gas-liquid system [22]:

$$\bar{H} = \rho V^2 / \rho_m V_m^2 = (1 - \xi^{1.5})^3, \quad \xi = Y/b.$$

Here Y and Y_m are coordinates of the point in question within the section and the corresponding point on the jet axis; b , radius of the jet in this section; and ΔP , ρV^2 , ΔP_m , $\rho_m V_m^2$, excess pressures and dynamic velocities at the points Y and Y_m . The results obtained agree well with the data in [7, 19, 20, 22].

Figure 2 shows empirical relations of the change in the dynamic velocity and excess pressure along the axis of a jet propagating in a liquid and in a gas according to our data and the data in [7, 19]. We should note the unique character of the curves for the gas-gas and gas-liquid systems. However, the heavy outer medium in the gas-liquid system causes a more rapid decrease in dynamic velocity compared to the submerged gas jet. At the same time,

[†]The function $\bar{P}_1^* = f(\bar{X}_1)$ was obtained by the authors on sonic bottom nozzles ($M_a \leq 1$) at $P_0 = (1.7-6.8) \cdot 10^5$ Pa.

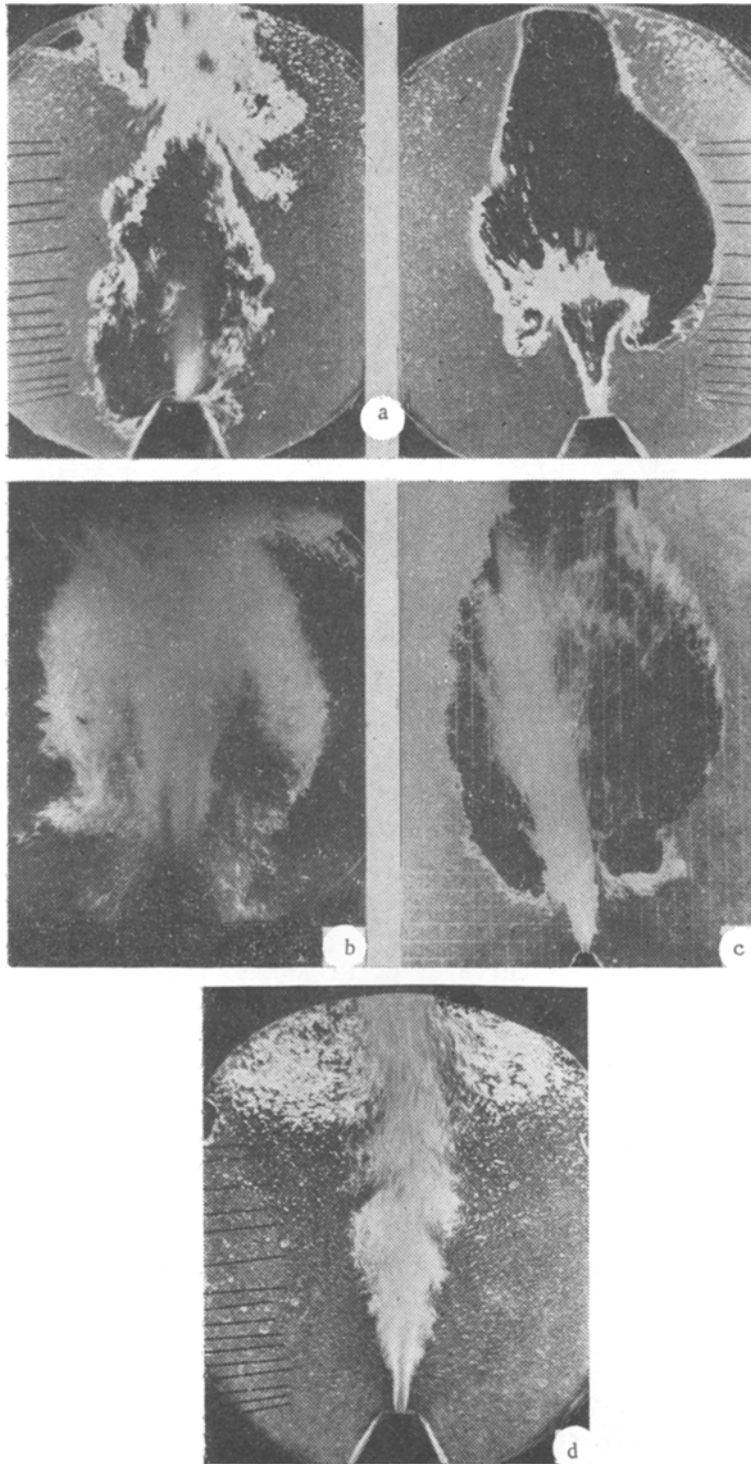


Fig. 1. Fragments of a film of the interaction of slightly (a-c) and strongly (d) assimilable gas jets with a liquid: a) $P_0 = 1.1 \cdot 10^5$ Pa, pulsative regime, $A \approx 0$, air-water; b) impingement of cavity on nozzle; c) surfacing of cavity: $P_0 = 3.5 \cdot 10^5$ Pa, regime of "single reverse shocks," $A \approx 0$; d) $P_0 = 4.5 \cdot 10^5$ Pa, regime of "shockless discharge," $A = 440$, HCl + water. Bottom plane nozzle $(2.5 \times 8) \cdot 10^{-3}$ m in cross section.

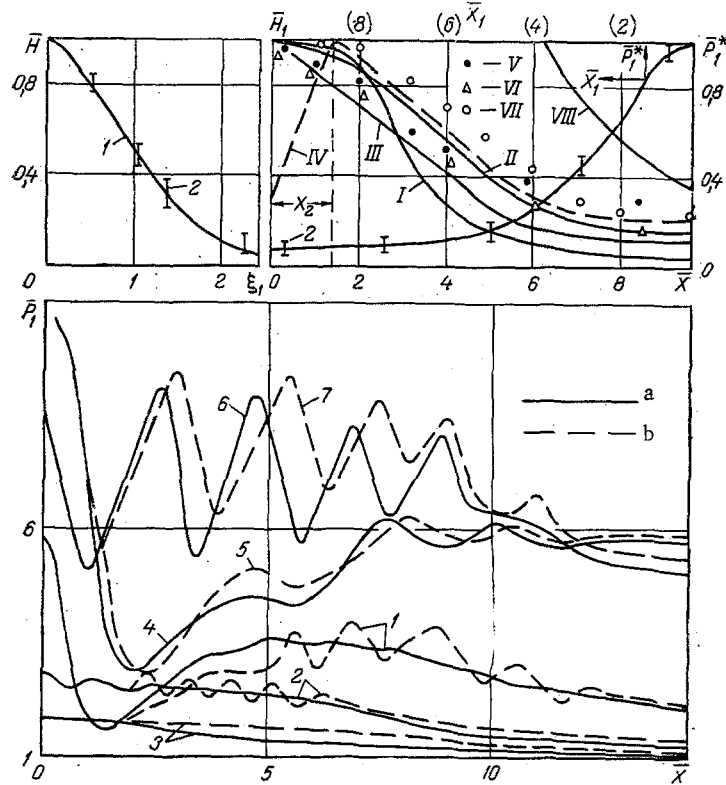


Fig. 2. Change in dimensionless values of the dynamic velocity \bar{H} across the jet and the dynamic velocity \bar{H}_1 , and excess pressure \bar{P}_1 , along the jet axis, as well as the dependence of the dimensionless pressure $\bar{P}_1^* = \Delta P_m / P_n$ on the coordinate $\bar{X}_1 = (X - X_p) / d_p$ for a slightly assimilated gas: $\bar{H} = f(\xi_1)$: 1 - curve of Abramovich [22]; 2) scatter of the test data, $P_0 = (1.5-4) \cdot 10^5$ Pa, $d_0 = 10 \cdot 10^{-3}$, lateral nozzle, $M_\alpha \leq 1$; $\bar{H}_1 = f(\bar{X})$: I) curve of G. N. Abramovich [7]; II) $V_\alpha = (150-\alpha)$ m/sec, $d_0 = 20 \cdot 10^{-3}$ m; III) $V_\alpha = (150-\alpha)$ m/sec, $d_0 = 12 \cdot 10^{-3}$ m, bottom nozzle, $M_\alpha \leq 1$ [19]; IV-VI) $V_\alpha = (40-105)$ m/sec, $d_0 = 10 \cdot 10^{-3}$, IV) bottom hole, V, VI) bottom nozzle [7]; VII) $V_\alpha = 280$ m/sec, $d_0 = 6 \cdot 10^{-3}$ m, bottom nozzle, $M_\alpha \leq 1$, data of authors, air (nitrogen)-water; VIII) gas jet in a gas [22]; $\bar{P}_1 = f(\bar{X})$: a) gas-liquid; b) gas-gas; 1-3) bottom sonic nozzles, $d_0 = 6 \cdot 10^{-3}$ m, $M_\alpha \leq 1$, data of authors [1) $P_0 = 5.8 \cdot 10^5$ Pa; 2) $2.9 \cdot 10^5$; 3) $1.7 \cdot 10^5$]; 4-7) lateral Laval nozzles, $d_0 = 8 \cdot 10^{-3}$ m [20] [4) $M_\alpha = 2.1$, $n = P_\alpha / P_f = 3$; 5) $M_\alpha = 1.95$, $n = 3.2$; 6) $M_\alpha = 2.6$, $n = 1$; 7) $M_\alpha = 2.5$, $n = 1$].

depending on $V_\alpha(P_0)$ and d_0 , there are deviations of the test values of \bar{H}_1 from the theoretical curve of Abramovich for the main section of the gas jet in the liquid [22]. Together with this, it can be seen from Fig. 2 that analysis of the test data in the form of the relation

$$\bar{P}_1^* = \Delta P_m / \Delta P_p = f[(X - X_p) / d_p],$$

where X_p , d_p , and ΔP_p are the coordinates of the beginning of the transitional section of the jet, the jet diameter, and the pressure on the jet axis in this section, made it possible to obtain a universal relation [23] for sonic bottom nozzles with $d_0 = (6-10) \cdot 10^{-3}$ m at $P_0 = (1.5-9) \cdot 10^5$ Pa. It should be kept in mind that $\rho_{\max} V_{\max}^2 = \rho_\alpha g V_\alpha^2$ for discharge from Laval nozzles and for subcritical sonic-nozzle regimes. For holes and supercritical sonic-nozzle regimes, $\rho_{\max} V_{\max}^2 > \rho_\alpha g V_\alpha^2$, and this is achieved in the section X_2 (Fig. 2).

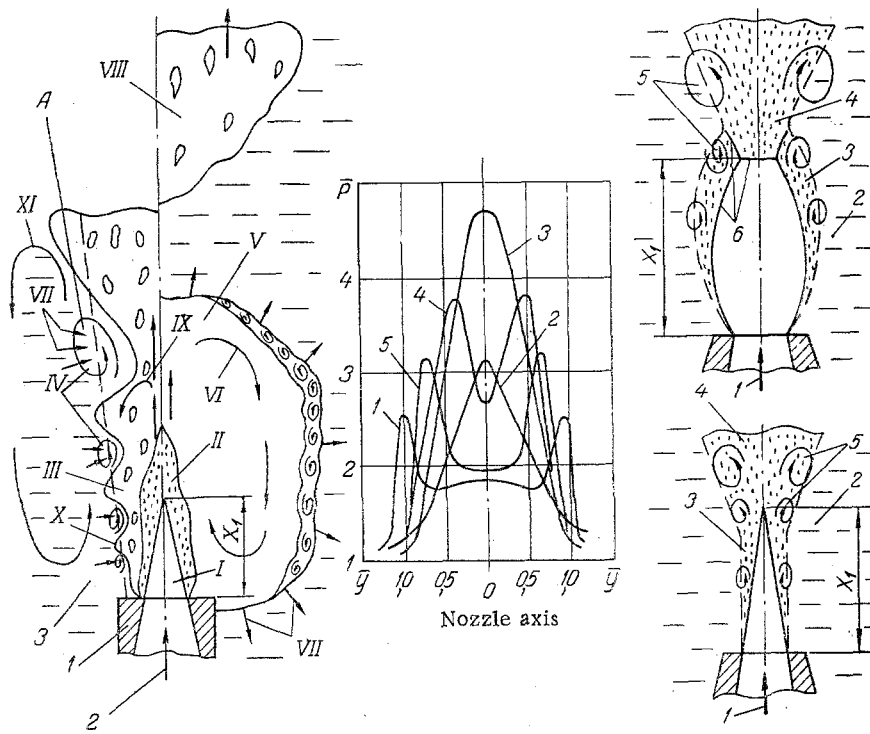


Fig. 3. Dynamic models of the interaction of jets of slightly and strongly assimilated gases with a liquid and the dependence of the excess pressure in the jet $\bar{p} = \Delta P/P_f$ on the coordinate $\bar{y} = 2Y/d_0$ for the strongly assimilated gas: 1-5) vapor-water, $T_g = 100^\circ\text{C}$, $T_q = 18^\circ\text{C}$ [26] and ammonia-water, $A = 710$, our data for $P_0 = 1.5 \cdot 10^5$ Pa: 1) $\bar{X} = X/d_0 = 0.25$; 2) $\bar{X} = 2$; 3) 1; 4) 0.6; 5) 0.4.

As can be seen from Fig. 2, studies of the initial section of a jet from a sonic nozzle, based on metallurgical practice, showed the similarity of the excess-pressure fields for gas-gas and gas-liquid systems. At supercritical discharges, in sonic nozzles, as in Laval nozzles [20], the wave structure of the flow is preserved and the profile is typical of a submerged gas jet (Fig. 2). However, the effect of the liquid leads to the creation of a developed two-phase boundary layer with bottom-lateral jets and to smoothing and more rapid erosion of the wave structure. The gasdynamic section on the whole is shorter, and during injection the shape and dimensions of the jumps may change.

Evaluation of the content of liquid phase in the flow showed the presence of a purely gaseous core of length $x_1 \leq (1-2)d_0$ for subcritical regimes and $x_1 \leq (3-10)d_0$ for supercritical regimes. The shape of the core can be seen in Fig. 3. In the case of strong assimilation ($A \geq 100-60$), the surface of the gaseous core is the boundary of the region of gas absorption by the liquid (Figs. 1, 3).

For subsonic axisymmetric jets, the gas core is a convergent cone and the maximum diameter of the jet, close to the diameter of the nozzle, is reached near the nozzle edge. With supercritical discharge from a sonic nozzle, the wave structure of the gas jet in the liquid and in the gas is similar, and the boundaries of the gaseous core in the liquid are close to the boundaries of the submerged gas jet. The greatest diameter of a jet undergoing assimilation in a liquid and the distance to this station can be evaluated from well-known relations for free gas jets [24]. The length and diameter of the region of interaction for strongly assimilated jets are an order lower than for a similar unassimilated jet [5], and are determined by the values $\bar{P} = P_f/P_0$ for $A \approx \text{const}$ and by the values of A for $\bar{P} \approx \text{const}$ [6, 25].

It can be seen from Fig. 3 that there is an especially sharp increase in excess pressures (dynamic velocities) at the boundary of the assimilation cone. The absolute values of these quantities increase from the nozzle edge to the apex of the cone. The peaklike increase in ΔP ($\rho V^2/2$) is due (with the retention of a profile typical of submerged gas jets right up to the surface of the assimilation cone) to the appearance of a heavy phase in the thin boundary layer. This phase consists of ejected liquid and products of chemisorption of the

gas. The flow is highly agitated beyond the apex of the cone. This turbulent region is not gas, but the main (carrying) part of the liquid, with the inclusion of condensate (for vapor), chemisorption products, and incompletely assimilated gas bubbles. This intensive agitation leads to rapid expansion of the flow beyond the apex of the cone (90-120°) and to rapid decay of the jet flow.

A decrease in the values of $A < 60-100$ (for vapor with $T_q > 40^\circ\text{C}$) leads to incomplete assimilation of the gas. In the interval $A = 20-100$ (for vapor with $T_q = 40-90^\circ\text{C}$), the profiles of excess pressure and dynamic velocity are restructured from those typical of complete assimilation to the corresponding flow of slightly assimilated and unassimilated gases. The above-examined structure of the interaction region is similar for all of the mechanisms of assimilation studied: absorption, chemisorption, and phase transformation.

Thus, excluding the low-velocity regime of gas movement at the nozzle edge, it may be concluded that the gas leaves a submerged nozzle and expands into a liquid in accordance with the laws of turbulent jet flow. However, the analogy with the gas-gas system is valid only for the internal region of interaction. On the whole, the flow is nonsteady, and under certain injection conditions it is unstable. The differences between the gas jet in the liquid and the heterogeneous turbulent systems examined in [16] and the gas-gas systems examined in [17, 22] stems from the specifics of the peripheral region of the flow and is connected with the dynamics of the boundary layer.

Mechanism of Interaction in a Gas-Liquid System. Studies of plane jets showed that the dynamics of the external region are connected with the appearance and development of systems of turbulent eddies of different scales. Due to the instability of the weak turbulent eddies relative to small perturbations, large-scale turbulence may be generated [27]. As can be seen from Fig. 1, such a process is characterized by ejection flows of the liquid phase into the eddy. Since the density of the liquid is a thousand times greater than the density of the gas, and since the apparent additional mass of the jet reaches $G_q \approx (100-150)G_g$, the appearance of a large-scale gas-liquid eddy causes transverse perturbation of the flow in this section. The asymmetry of the flow leads to the appearance and growth of local hydraulic resistance, which is equivalent to a reduction in the through cross section of the jet. With a constant discharge from the nozzle, this leads to the accumulation of gas in the region between the nozzle edge and the section of the initial perturbation - to the formation of a large gas volume, or cavities. In supercritical injection regimes, the constriction of the through section of the jet may lead to the appearance of a reverse eddy flow (part of the gas, reflected from the barrier, moves toward the nozzle edge) (Figs. 1, 3).

Particularly large turbulent eddies, which cause the greatest transverse perturbations of the jet, may lead to separation of the flow and the formation of discrete gaseous and two-phase volumes. In this case, all of the gas leaving the nozzle is brought into the circulating flow in the cavity. The rate of growth of the cavity increases sharply, as does the agitation of its two-phase boundaries. Movement of the front of the cavity when the jet is moving into it at near-sonic or supersonic velocities causes a hydraulic shock in the liquid. At the moment the cavity reaches the nozzle and the wall of the lance, the high-velocity gas flow exerts a strong mechanical force on the nozzle and wall. The aggregate effect of these factors leads to the "reverse shock" typical of bottom-lateral lances, which breaks the lance.

The intensity of the "reverse shocks" increases with an increase in P_0 and V_a . However, the resistance of the jet to transverse perturbations **also** increases here, and there is a decrease in the apparent additional mass of the jet. The latter is manifest in a decrease in the frequency of appearance of the cavities and disruption of the periodicity of their appearance and, thus, less-regular "reverse shocks." After it moves away from the nozzle, the cavity surfaces as a result of buoyancy. The gas jet from the nozzle again moves deeper into the liquid, which leads to the appearance of a new system of turbulent eddies and a repetition of the above-described process (see Fig. 1).

In the case of a low-velocity turbulent gas jet, due to the high instability with respect to transverse oscillations, the continuity of the flow is disrupted close to the nozzle edge - the flow **breaks** down, accompanied by the formation of large gas bubbles. The periodicity of the process of initiation and destruction of a system of turbulent eddies in the boundary layer, noted in [27], leads to the appearance of a mixed flow: in the vicinity of the nozzle, either a stable jet or a pulsating bubble is periodically formed. The section in which the flow breaks down is determined by the energy reserves of the jet and shifts from

the nozzle edge downstream with an increase in P_0 and V_α . We should emphasize the differences in the conditions of appearance of the regimes of mixed flow and "reverse shocks." The latter is characteristic of a section of turbulent flow in which the energy reserves of the jet are adequate to maintain a stable flow, and they are random in nature.

As can be seen from Fig. 1, gas assimilation leads to a decrease in the intensity of the turbulent eddies in the boundary layer of the gas jet. The ejection process becomes more stable and uniform and slightly dependent on individual large-scale eddies. The most powerful eddies, developing in the liquid, no longer have an effect on the stability of the gas flow. Thus, regardless of the assimilation mechanism, gas assimilation stabilizes the flow. In the case of intensive assimilation ($A \geq 60-100$), the flow may be regarded as quasisteady. Study of the process of interaction of the gas jet with the liquid allowed us to construct dynamic models of the interaction region which take into account the degree of assimilation of the gas (Fig. 3).*

The model for weak gas assimilation includes: 1) nozzle; 2) gas; 3) liquid; I) gaseous core of length X_1 ; II) gas-liquid region (drop occlusions); III) liquid-gas region (bubble occlusions); IV) system of turbulent eddies; V) pulsating cavity; VI) circulating flow of gas in the cavity; VII) liquid brought in motion by the eddies and the boundary of the cavity; VIII) gas volume separated from the jet; IX) part of gas under the influence of the intensive turbulent eddy A, turning in the direction of the nozzle and forming a circulating flow in the cavity; X) hypothetical boundary of jet; XI) mean circulating flow in the liquid volume.

The model for strong gas assimilation includes: 1) gas; 2) liquid; 3) two-phase boundary layer; 4) flow of liquid with occlusions of products of chemisorption of the gas and nonassimilated gas bubbles; 5) system of turbulent eddies; 6) system of shock waves, determined by $n = P_\alpha/P_f, M_\alpha$.

Discharge Regimes. In accordance with the above-examined flow dynamics, we propose two basic regimes of discharge: bubble and jet. The bubble regime takes place at high-speed discharges of the gas $V_\alpha \leq 2-30$ m/sec and, as will be shown below, corresponds to laminar flow of the gas. The jet regime is associated with turbulent discharge of the gas from the nozzle. In turn, the instability of the boundary layer of the gas jet entering the liquid further differentiates the jet regime for bottom and lateral nozzles into four other regimes: pulsating regime, transitional regime, regime of single reverse shocks, and a pure jet regime - a regime of shockless discharge. For submerged top nozzles it is expedient to subdivide the jet regime into a pulsating regime and a pure jet regime - a regime in which a stable cavity is formed.

The bubble regime is associated with the periodic formation and separation, at the nozzle edge, of discrete gas bubbles. The gas-liquid interface in this case is smooth. The shape of the bubbles depends on the location of the nozzle edge, adhesion of the liquid to the material of the nozzle and the lance wall, and the value of the contact angle. The bubble regime is characterized by linear dependence of the frequency of bubble separation on the injection regimes (P_0, V_α, G_g). This linear dependence is violated only at very low values of these parameters and near the boundaries of the regime (Fig. 4).† The main determining criteria are $\bar{P} = P_f/P_0, \bar{V} = V_\alpha/\alpha$. The tests also showed (Fig. 4) the significant role of the physical parameters of the liquid (ρ_q, μ_q, σ_q). At the same time, gas assimilation A does not affect the frequency of formation and separation or the dimensions of the gas bubbles formed at the nozzle edge.

The boundary of the regime is characterized by the establishment of $\tau \approx \tau_{\max}$ and is realized at $I = 0.01-0.05H$, where $I = \rho_g \alpha V_\alpha^2 F_\alpha + (P_{ag} - P_f)F_\alpha$ is the momentum of the gas jet, and at the numbers $Re = V_\alpha d_0 / \nu_g = 500-2500$ for all of the injection conditions studied. Thus, the boundary of the bubble regime is determined by the transition from laminar flow of the gas at the nozzle edge to turbulent flow. To allow for the effect of d_0 , which occurs in examining the function $\tau = f(P_0, V_\alpha, G_g)$, the following relation is recommended:

*For the model of the interaction of a slightly assimilable gas, that part of the scheme left of the axis corresponds to the development of a stable two-phase jet in the liquid. The right part corresponds to development of the cavity.

†Since $V_\alpha = \alpha (M_\alpha \leq 1)$ for sonic nozzles with a supercritical discharge, then $V_\alpha = V_h$ - the hypothetical velocity - is determined by the values $P = P_f/P_0$.

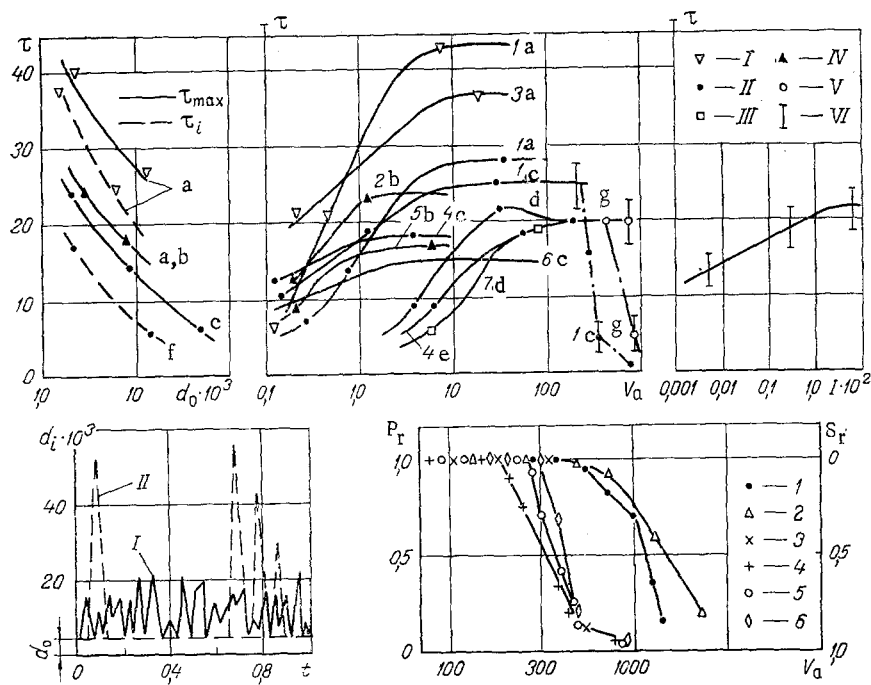


Fig. 4. Dependences of the frequency of formation and separation of bubbles near the nozzle edge τ (Hz) on the gas discharge velocity V_a (m/sec), the impulse of the jet $I \cdot 10^{-2}$ (N), and the nozzle diameter d_0 , 10^{-3} m, as well as the instantaneous values of the diameter of the flow at the nozzle edge d_i , 10^{-3} m, during injection t , and the dependence of the probability of realization of the "shockless discharge" and "pulsative" regimes on the rate of discharge of the gas from the nozzle V_a (m/sec), $\tau = f(d_0, V_a, I)$: I) nitrogen-ethanol; II) air (nitrogen)-water; III) air (nitrogen)-glycerin; IV) argon-cast-iron; V) nitrogen-mercury; VI) scatter of experimental data [1] $d_0 = 2 \cdot 10^{-3}$ m; 2) $3 \cdot 10^{-3}$; 3) $4 \cdot 10^{-3}$; 4) $6 \cdot 10^{-3}$; 5) $8 \cdot 10^{-3}$; 6) $10 \cdot 10^{-3}$; 7) $0.5 \cdot 10^{-3}$; a) [1]; b) [2]; c) our data; d) [28]; e) [3]; f) [7]; g) [10]; $d_i = f(t)$ and the probability $f(V_a)$: I) $\bar{P} = P_f/P_0 = 0.5$; II) $\bar{P} = 0.26$, $d_0 = 2 \cdot 10^{-3}$ m, our data [1, 2) mercury-nitrogen [10]; 3) water-nitrogen [4]; 4-6) water-air, our data; 1, 3) $d_0 = 3 \cdot 10^{-3}$ m; 2) $1 \cdot 10^{-3}$; 4) $4 \cdot 10^{-3}$; 5) $2 \cdot 10^{-3}$; 1-5) bottom nozzles; $Ma \leq 1$; 6) $d_0 = 4 \cdot 10^{-3}$ m, lateral nozzle); P_r) pulsative regime; S_r) shockless regime.

$$\bar{V}_a^* = V_a^* a = 100 / (0.44 \bar{d}_0^2 + 13.05 \bar{d}_0 + 4.4), \quad \bar{d}_0 = d_0 / d_{01}, \quad d_{01} = 1 \text{ m}^2$$

characterizing the boundary of the bubble regime.

The pulsative regime, as the previous regime, is connected with the formation of discrete gas volumes and the retention of jet flow in the central region of the flow. The pulsative regime is characterized by a disruption in the continuity of the flow, which corresponds to the above-examined mixed flow. The visible difference from the bubble regime is the presence of a gas bridge at the nozzle edge. These gas bridges, or "stems," have a complex shape which changes with time. The stems become longer as the discharge is intensified. The gas volume is intensively forced through the stem until it is separated. The stem is based on the jet profile examined earlier.

Inertial forces govern the process in the pulsative regime. Bubbles extended along the axis - ellipsoids - are formed with any location of the nozzle. Instability of the jet leads to regular pulsation of the flow with the frequency $\tau \approx \tau_{max}$, while the presence of reverse eddies leads to spreading of the bubble over the nozzle and the lance wall. The latter increases the diameter of the flow at the nozzle edge to $(10-15)d_0$. The completed studies showed the absence of an appreciable effect ($\leq 10-15\%$) of the physical parameters of the gas and liquid on the frequency characteristics of the process. The empirical approximation of the boundary of the pulsative regime for highly assimilable gases ($A \geq 40-60$) has the form

$$\bar{P}^* = P_f/P_0 = \sqrt{\frac{A+14}{4217}} + 0.57.$$

At $A < 40-60$, beyond the boundary of the pulsative regime we took values of \bar{P} and \bar{V}_α corresponding to the beginning of disruption of the regularity of the pulsations at the nozzle edge (Fig. 4). According to our data, the pulsative regime is realized at $(0.99-0.9999) \geq \bar{P} \geq (0.78-0.55)$; $(0.008-0.1) \leq \bar{V}_\alpha \leq (0.6-1.0)$. In the case of more intensive injection, the flow along the axis consists of two regions: a stable jet flow with a characteristic geometry and pulsating at a frequency of 10-20 Hz, and regions of discrete gas bubbles, the dimensions and shape of which change continuously in connection with the division and coalescence of the gaseous and two-phase volumes. The jet section is randomly discontinuous, as noted above, and this leads to the formation of cavities. Due to this, the instantaneous values of the flow diameter at the nozzle edge change from $(1-3)d_0$ in the formation of the jet to $(15-30)d_0$ with the approach of the cavity. With an increase in P_0 and V_α , the regularity of the appearance of the cavities and the corresponding "reverse shocks" is increasingly disturbed, the frequency decreases, and the diameter of stable flow at the lance edge approaches the diameter of the outlet section of the nozzle. In fact, both the pulsative and pure jet (shockless discharge) regimes are realized alternately near the nozzle edge.

Such a flow is best examined from the point of view of the probability of the existence of unstable discrete gas volume or a continuous jet at the lance edge. Figure 4 reflects the results we obtained on model media and the results obtained in [9, 10] with mercury. On the basis of these results, we tentatively divided the discharge process into two regimes: transitional and single reverse shocks.

The transitional regime is characterized by a 100-200% probability of realization of the pulsative regime (100% corresponds to the boundary of this regime). The frequency of appearance of gaseous volumes - cavities - changes with an increase in P_0 from $\tau \approx \tau_{\max}$ to $\tau = 4-6$ Hz.

For the regime of single reverse shocks, the probability of pulsative processes is less than 20-25% (a stable jet exists at the nozzle edge for more than 80-75% of the injection time). This regime is characterized by abrupt random pulsations of the flow - "reverse shocks." The frequency of these shocks decreases to hertz at $\bar{P} < 0.3-0.25$ and to tenths of a hertz at $\bar{P} < 0.1-0.05$. Thus, the region of existence of the transitional regime is $(0.78-0.55) \geq \bar{P} \geq (0.3-0.25)$, while the regime of single reverse shocks exists at $\bar{P} < (0.25-0.3)$. Since the appearance of the gaseous volumes (cavities) is random in nature, neither d_0 nor the physical characteristics of the media were observed to have an effect on the frequency characteristics of the process.

Highly assimilable gases ($A > 40-60$) are characterized by only two limiting (pulsative and pure jet) regimes. The lack of the bubble regime is connected with the strong assimilation of the gas by the melt and flow of the liquid into the nozzle and gas line at low P_0 and V_α , which is intolerable in practice. The lack of the "transitional" and "single-reverse-shock" regimes is due to the nearly instantaneous transition from a discrete flow to a continuous jet.

Thus, the results we obtained make it possible to determine the region of interaction in a gas-liquid system for all injection regimes and degrees of gas assimilation. The results are valid for water, solutions, melts, and hot and cold gases.

NOTATION

$n = P_\alpha/P_f$, underexpansion of jet; $I = \rho_g \alpha V_\alpha^2 F_\alpha + (P_{ag} - P_f)F_\alpha$, impulse of the jet; $Re = Vd/\nu$, Reynolds number; V , flow velocity; d , diameter; ν , μ , kinematic and absolute viscosities; A , degree of assimilation (volume of the gas absorbed by a unit volume of the liquid); ρ , density; σ , surface tension; T , temperature; P , P_0 , pressure, pressure ahead of the nozzle; G , discharge; F , area; τ , frequency; $M_\alpha = V_\alpha/\alpha$, theoretical Mach number of nozzle; α , speed of sound; $P_f = P_{atm} + \rho_q gH$, hydrostatic pressure; H , height of column of liquid above nozzle; P_{atm} , pressure above surface; $d_\alpha = d_0$ for sonic (cylindrical and convergent) nozzles ($M_\alpha \leq 1$). Indices: g , gas; q , liquid; α , boundary of a regime; α , 0, outlet and critical sections of the nozzle; $\bar{H} = \rho V^2 / \rho_m V_m^2$; $\bar{H}_1 = \rho_m V_m^2 / \rho_{\max} V_{\max}^2$; $\bar{P}_n = \Delta P_m / P_f$, $\zeta_1 = Y/Y_c$, $\bar{X} = X/d_\alpha$, Y_c , coordinate of the point for which $\rho V^2 \approx 0.5 \rho_m V_m^2$.

LITERATURE CITED

1. Yu. A. Buevich and V. V. Butkov, "Mechanism of bubble formation in the discharge of a gas into a liquid from a circular opening," *Teor. Osn. Khim. Tekhnol.*, 5, No. 1, 74-83 (1971).
2. V. I. Berdnikov, A. M. Levin, and K. M. Shakirov, "Bubble size in the injection of metal," *Izv. Vyssh. Uchebn. Zaved., Chern. Metall.*, No. 10, 15-22 (1974).
3. N. A. Lebedinskaya, M. Z. Zhivov, E. I. Ezhov, et al., "Propagation of a horizontal gas jet into a heavy liquid," in: *Transactions of the "Gipronikel" Institute, Leningrad* (1973), Vol. 57, pp. 86-90.
4. G. P. Ivanov and Z. M. Kudryavtseva, "Study of the aerodynamics of assimilable and non-assimilable gas jets entering a liquid," in: *Steel Production [in Russian], Metallurgizdat, Moscow* (1960), pp. 297-316.
5. I. P. Ginzburg, V. A. Surin, A. A. Bagautdinov, et al., "Study of the discharge of a gas stream from a submerged nozzle into a liquid," *Inzh.-Fiz. Zh.*, 33, No. 2, 213-223 (1977).
6. V. A. Surin, V. K. Erofeev, A. S. Grigor'yants, et al., "Interaction of a gas jet with a liquid bath with different degrees of assimilation of the gas," *Inzh.-Fiz. Zh.*, 36, No. 3, 440-448 (1979).
7. A. S. Vasil'ev, V. S. Talachev, and V. P. Pavlov, "Laws of discharge of a gas jet into a liquid," *Teor. Osn. Khim. Tekhnol.*, 4, No. 5, 727-735 (1970).
8. A. V. Grechko, R. D. Nesterenko, and Yu. A. Kudinov, *Experience in Physical Modeling at a Metallurgical Plant [in Russian], Metallurgiya, Moscow* (1976).
9. A. N. Sherstnev and V. P. Savva, "Conditions of physical interaction of a gas jet with a liquid," in: *Scientific Transactions of the Leningrad Mining Institute, Vol. 7, Leningrad* (1975), pp. 56-61.
10. K. Mori, Ya. Odzava, M. Sano, and U. Fugita, "Tetsu to hagane," *J. Iron Steel Inst., Jpn.*, 61, No. 12, 98 (1975); 64, No. 11, 128-129 (1978); 65, No. 8, 10-18 (1979); 66, No. 3, 134 (1980); 66, No. 4, S162 (1980).
11. A. V. Spesivtsev, "Study of the interaction of an unassimilated gas jet with some melts in nonferrous metallurgy," *Author's Abstract of Candidate's Dissertation, Engineering Sciences, Moscow* (1973).
12. V. P. Savva, A. V. Spesivtsev, N. G. Kopaev, et al., "Distribution of the constituents of a converter bath during the injection of a copper-nickel matte," *Tsvetn. Met.*, No. 5, 18-20 (1980).
13. K. S. Prosvirin, V. I. Trubavin, and G. A. Shchedrin, "Structure and parameters of the reaction zone in the bottom injection of metal with oxygen," in: *Heat and Mass Transfer in Steelmaking Furnace Baths, Scientific Transactions of the MISiS, No. 120, Metallurgiya, Moscow* (1979), pp. 95-99.
14. V. I. Baptizanskii, V. I. Trubavin, and B. M. Boichenko, "Interaction of a gas jet with liquid metal in bottom-blown oxygen converters," *Izv. Vyssh. Uchebn. Zaved., Chern. Metall.*, No. 10, 33-38, (1980); No. 12, 22-26 (1980).
15. A. G. Chernyatevich, B. I. Shishov, and G. M. Solomon, "Interaction of an oxygen jet with a metallic bath," *Izv. Vyssh. Uchebn. Zaved., Chern. Metall.*, No. 2, 30-34 (1980).
16. A. I. Nakorchevskii, *Heterogeneous Turbulent Jets [in Russian], Naukova Dumka, Kiev* (1980).
17. L. A. Vulis and I. N. Terekhina, "Propagation of a turbulent gas jet into a medium of a different density," *Zh. Tekh. Fiz.*, 26, No. 6, 1277-1291 (1956).
18. L. M. Efimov, "Hydrodynamics of a submerged gas jet," *Staleplavil'n. Proizvod.*, No. 2, 22-27 (1974).
19. B. F. Glikman, "Gas jet in a liquid," *Izv. Akad. Nauk SSSR, Otd. Tekh. Nauk, Energ. Avtom.*, No. 2, 135-136 (1959).
20. M. G. Moiseev, "Discharge of a gas into a liquid through a Laval nozzle," *Inzh.-Fiz. Zh.*, 5, No. 91, 81-84 (1962).
21. Ikeda Ryuka, Taga Masayuki, Aoki Kenro, et al., "Features of the behavior of a gas jet in a liquid and during refining," *Tetsu hagane, J. Iron Steel Inst., Jpn.*, 65, No. 8, A141-A144 (1979).
22. G. N. Abramovich, *Theory of Turbulent Jets [in Russian], Fizmatgiz, Moscow* (1960).
23. V. E. Davidson, E. Ya. Kapustin, and V. N. Evchenko, "Gas jet being discharged into a liquid," *Gidroaeromekh. Teor. Uprugosti*, 27, 85-95 (1982).
24. V. N. Glaznev and Sh. Suleimanov, *Gasdynamic Parameters of Slightly Underexpanded Free Jets [in Russian], Novosibirsk, Nauka* (1980).
25. V. A. Surin, V. K. Erofeev, O. N. Zasukhin, et al., "Hydrodynamics of a gas jet with different degrees of its assimilation by a liquid," in: *Heat and Mass Transfer in Steel-Making Furnace Baths, Scientific Transactions of the MISiS, No. 120, Metallurgiya, Moscow* (1979), pp. 42-46.

26. B. F. Glikman, "Experimental study of the condensation of a vapor jet in a space filled with a liquid," *Izv. Akad. Nauk SSSR, Otd. Tekh. Nauk, Energ. Avtom.*, No. 1, 39-44 (1959).
27. A. A. Townsend, "Mechanism of penetration of free turbulent jets," *Mechanics, Periodical Collection of Translations*, No. 4, 61-90 (1968).
28. M. B. Aizenbud and V. V. Dil'man, "Problems of the hydraulics of chemical reactors for gas-liquid systems," *Khim. Promst.*, No. 3, 51-56 (1961).

EFFECT OF PARTICLES ON THE RATE OF TURBULENT TRANSPORT
OF A DUST-LADEN GAS

I. V. Derevich, V. M. Eroshenko,
and L. I. Zaichik

UDC 532.529

Simple approximations in equations of single-point second moments were used to analyze the effect of particles on the intensity of pulsative motion in a nonuniform turbulent flow.

It is well known that even a small concentration of a solid-particle impurity in a turbulent gas flow has a significant effect on the turbulent pulsations of the gas or of the gaseous suspension as a whole [1-7]. Heavy inertialess particles may result in a decrease in turbulence energy due to buoyancy [1, 5]. Light inertialess particles change the turbulence spectrum [2, 5]. The latter particles lead to additional dissipation of the turbulence energy, the magnitude of this dissipation being comparable to the dissipation in a non-dust-bearing gas [3, 6, 7].

The present work examines the turbulent flow of a gas with solid particles which do not interact with one another; in the absence of body forces, the particles interact with the flow only as a result of viscous drag. We obtained closed expressions to correlate the pulsations of particle and gas velocity in the nonuniform flow. Allowing for these expressions, we constructed the system of equations for the second moments of the pulsations of the velocity of the dust-laden gas and used this system as a basis for studying the effect of particle inertia and concentration on the rate of turbulent transport.

1. The following equations of motion of the gas and particles are used to calculate turbulent gas flows with particles:

$$\frac{\partial U_i}{\partial t} + U_k \frac{\partial U_i}{\partial x_k} = -\frac{1}{\rho_1} \frac{\partial P}{\partial x_i} + \nu \frac{\partial^2 U_i}{\partial x_k \partial x_k} - C \frac{\rho_2}{\rho_1} \frac{1}{\tau} (U_i - V_i), \quad (1)$$

$$\frac{\partial V_j}{\partial t} + V_k \frac{\partial V_j}{\partial x_k} = \frac{1}{\tau} (U_j - V_j). \quad (2)$$

Equation (2) can be written in integral form:

$$V_j(x, t) = \frac{1}{\tau} \int_0^t ds \exp\left(-\frac{t-s}{\tau}\right) \left\{ U_j(x, s) - \tau V_k(x, s) \frac{\partial V_j(x, s)}{\partial x_k} \right\}. \quad (3)$$

We will represent all of the parameters characterizing the motion of the gas and particles in the form of the sum of the mean and pulsative (fluctuation) components. Then for the mean and pulsative components of particle velocity, respectively, we find from (3) that

$$\begin{aligned} \langle V_j(x, t) \rangle &= \frac{1}{\tau} \int_0^t ds \exp\left(-\frac{t-s}{\tau}\right) \left\{ \langle U_j(x, t-s) \rangle - \right. \\ &\left. - \tau \left[\langle V_k(x, t-s) \rangle \frac{\partial \langle V_j(x, t-s) \rangle}{\partial x_k} + \langle v_k(x, t-s) \rangle \frac{\partial v_j(x, t-s)}{\partial x_k} \right] \right\}, \end{aligned} \quad (4)$$

G. M. Krizhizhanovskii State Scientific-Research Institute of Energy, Moscow. Translated from *Inzhenerno-Fizicheskii Zhurnal*, Vol. 45, No. 4, pp. 554-560, October, 1983. Original article submitted July 5, 1982.